

[advances.sciencemag.org/cgi/content/full/7/4/eabe1174/DC1](https://advances.sciencemag.org/cgi/content/full/7/4/eabe1174/DC1)

## Supplementary Materials for

### **1-Methylnicotinamide is an immune regulatory metabolite in human ovarian cancer**

Marisa K. Kilgour, Sarah MacPherson, Lauren G. Zacharias, Abigail E. Ellis, Ryan D. Sheldon, Elaine Y. Liu, Sarah Keyes, Brenna Pauly, Gillian Carleton, Bertrand Allard, Julian Smazynski, Kelsey S. Williams, Peter H. Watson, John Stagg, Brad H. Nelson, Ralph J. DeBerardinis, Russell G. Jones, Phineas T. Hamilton, Julian J. Lum\*

\*Corresponding author. Email: [jjlum@bccancer.bc.ca](mailto:jjlum@bccancer.bc.ca)

Published 20 January 2021, *Sci. Adv.* 7, eabe1174 (2021)  
DOI: 10.1126/sciadv.abe1174

#### **The PDF file includes:**

Figs. S1 to S5

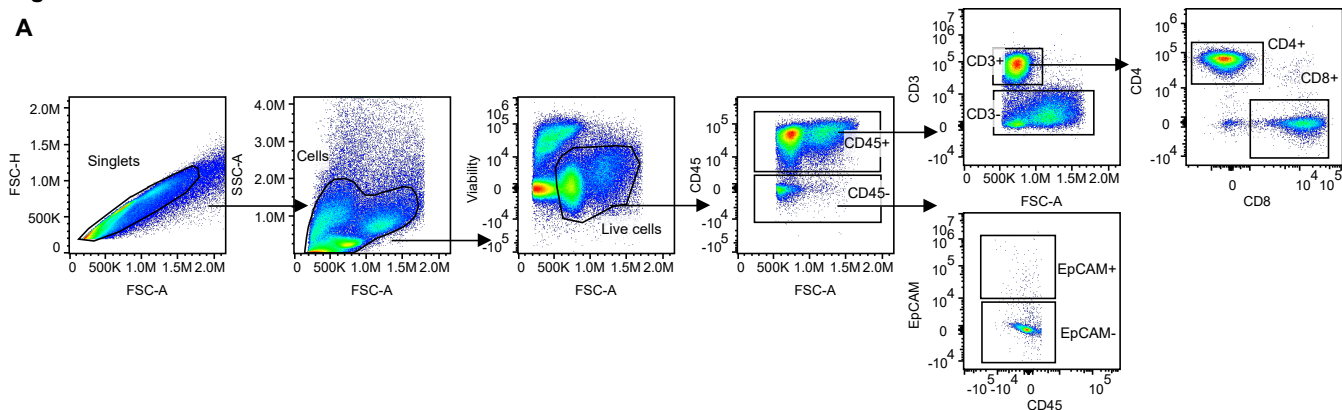
#### **Other Supplementary Material for this manuscript includes the following:**

(available at [advances.sciencemag.org/cgi/content/full/7/4/eabe1174/DC1](https://advances.sciencemag.org/cgi/content/full/7/4/eabe1174/DC1))

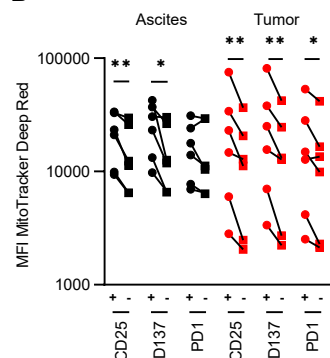
Tables S1 to S5

fig. S1

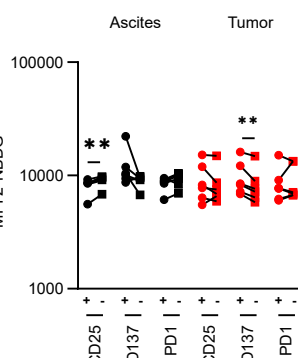
A



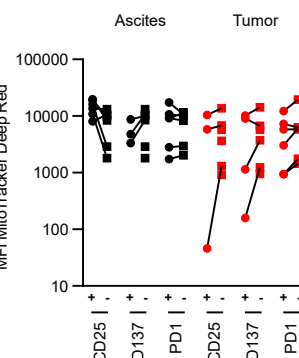
B



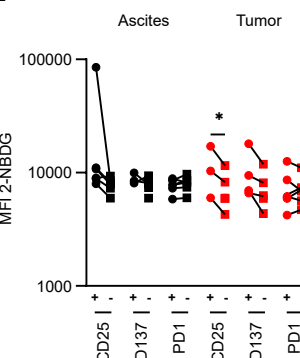
C



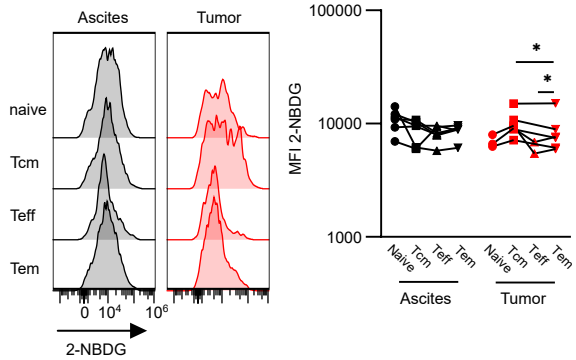
D



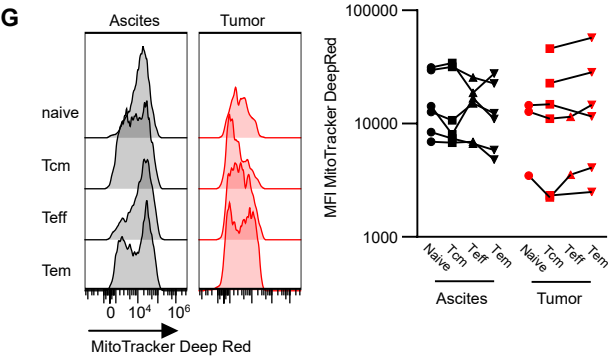
E



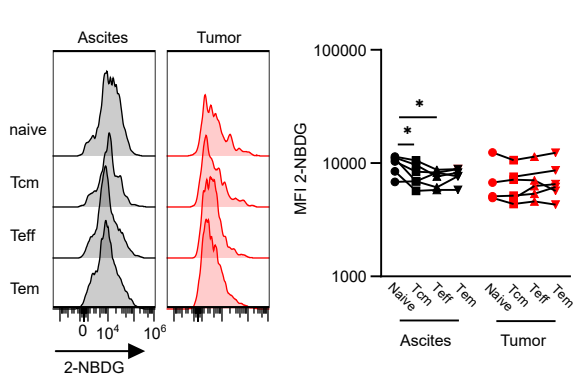
F



G



H



I

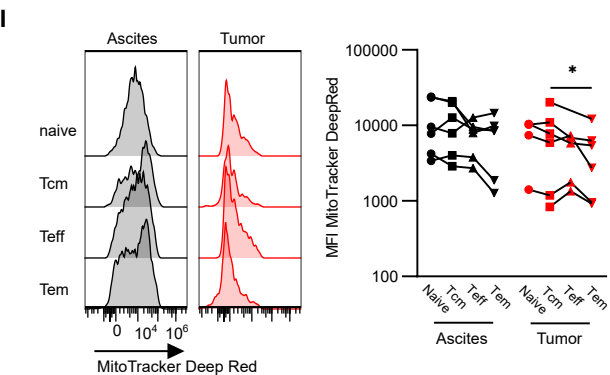


fig. S2

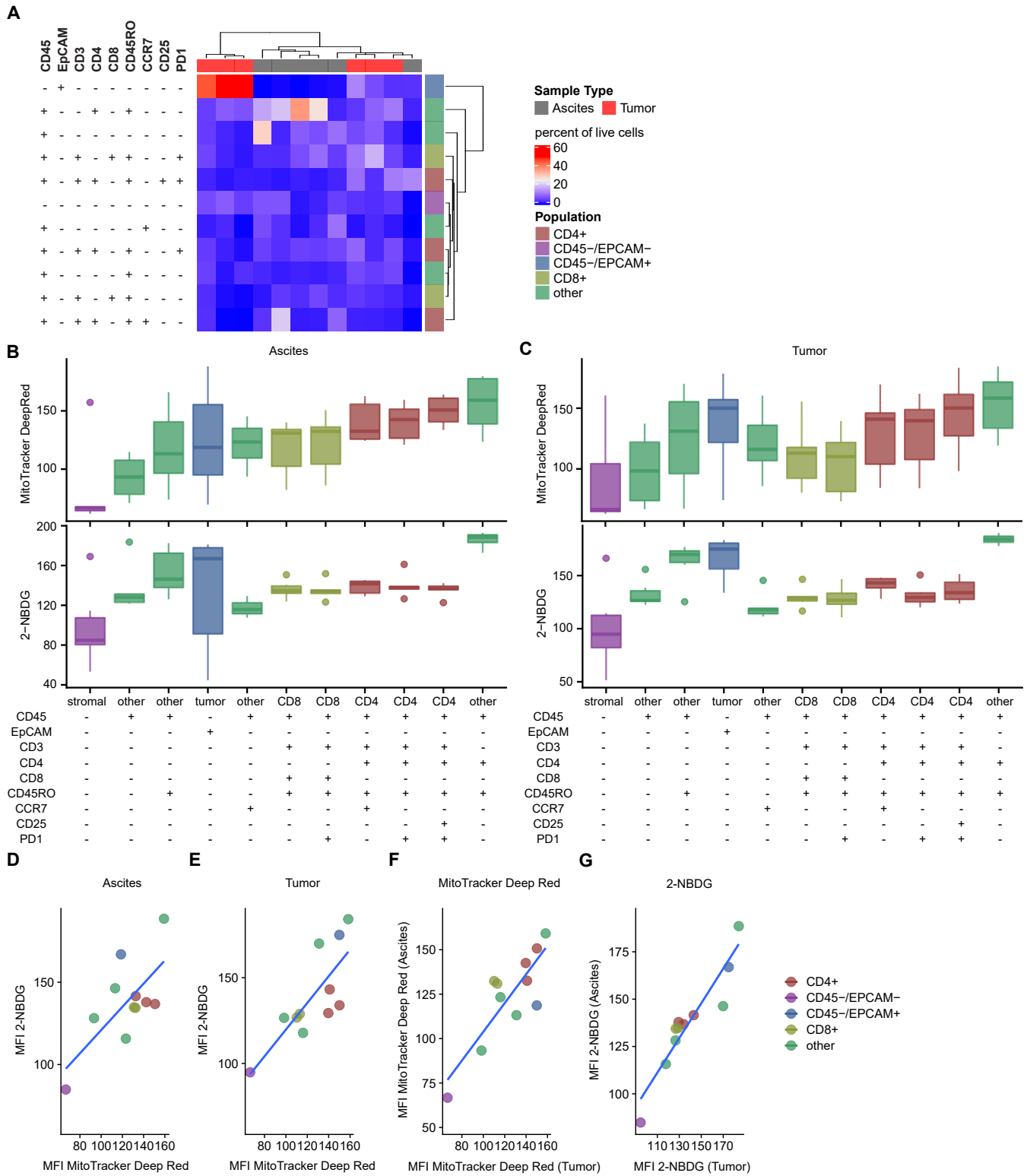
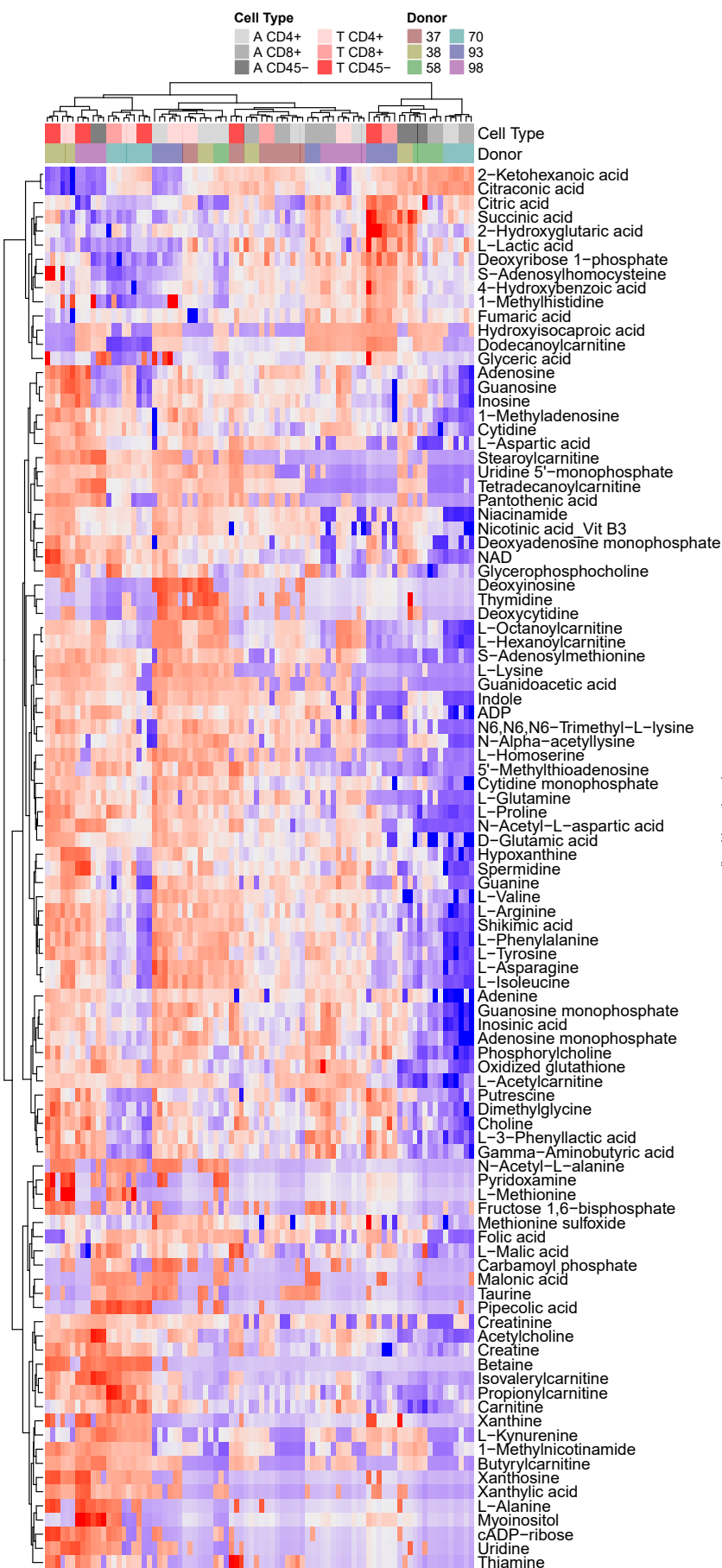
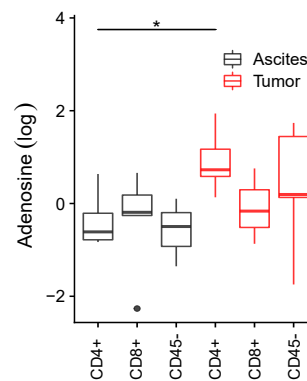


fig. S3

A



B



C

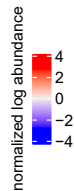
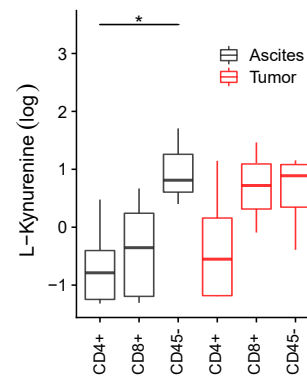
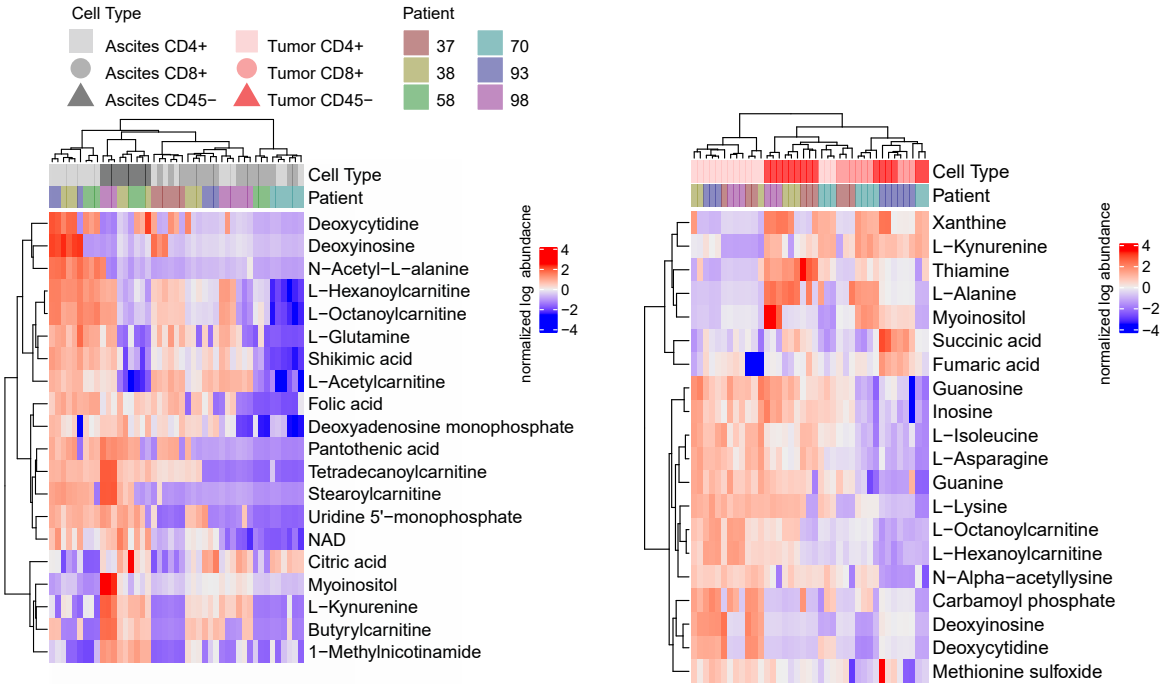


fig. S4

A



B

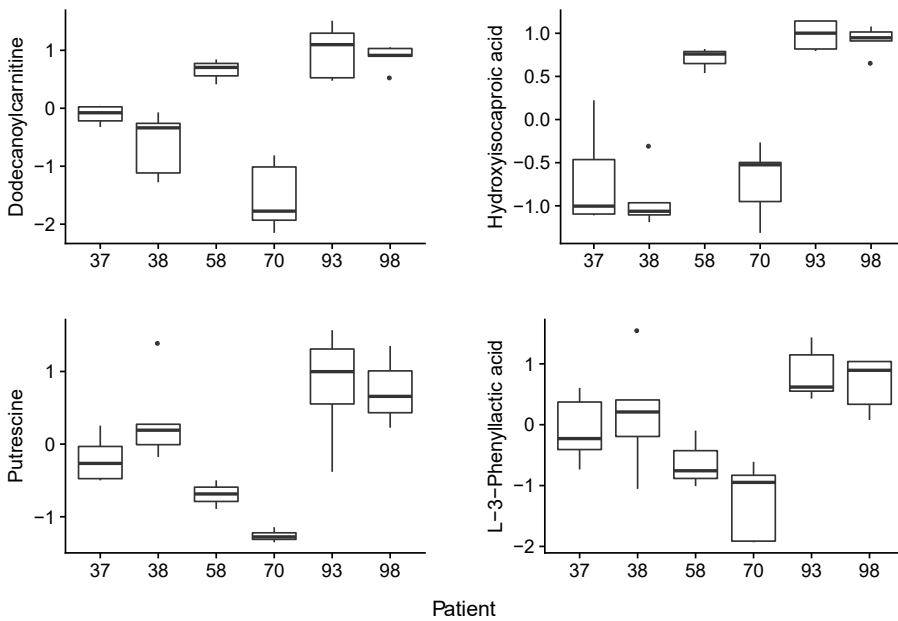
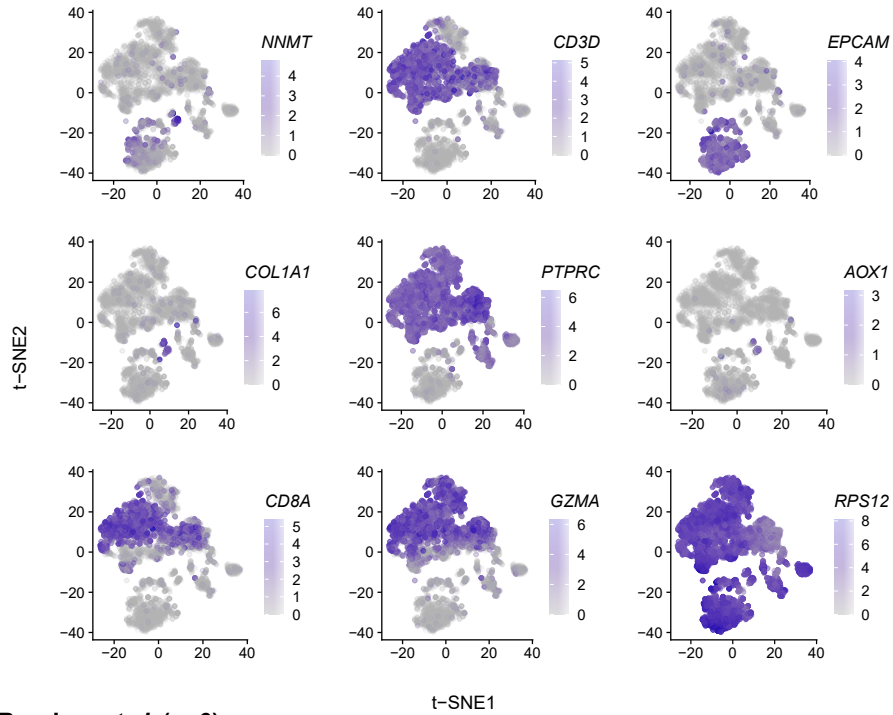
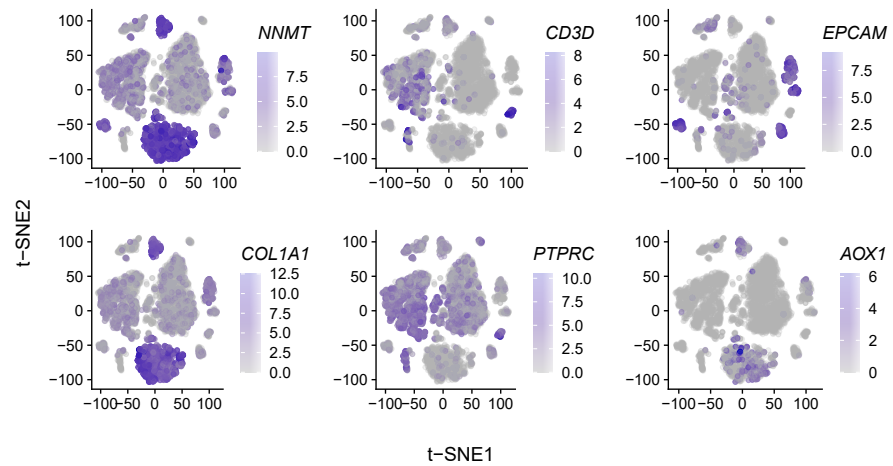


fig.S5

**A Kilgour et al. (n=3)**



**B Izar et al. (n=6)**



## SUPPLEMENTAL FIGURE LEGENDS

### **fig. S1. T cell metabolism is minimally impacted by expression of activation and differentiation markers.**

(A) Representative gating strategy for analysis by flow cytometry.

(B-C) Mitochondrial activity (B) and glucose uptake (C) of CD25, CD137 and PD1 +/- CD4+ T cells.

(D-E) Mitochondrial activity (D) and glucose uptake (E) of CD25, CD137 and PD1 +/- CD8+ T cells.

(F-G) Representative plot (left) and tabulated data (right) for glucose uptake (F) and mitochondrial activity (G) of naive, Tcm, Teff and Tem CD4+ T cells.

(H-I) Representative plot (left) and tabulated data (right) for glucose uptake (H) and mitochondrial activity (I) of naive, Tcm, Teff and Tem CD8+ T cells. p-values (\* $p < 0.05$ , \*\* $p < 0.01$ , \*\*\* $p < 0.001$ ) determined by paired t-test (B-I). Lines indicate matched patients (B-I). Fluorescence Minus One (FMO); Median Fluorescence Intensity (MFI); Central memory T cells (Tcm); Effector T cells (Teff); Effector memory T cells (Tem).

### **fig. S2. Automated analysis of metabolism and cell type by flow cytometry.**

(A) Heat map of cell type abundance.

(B-C) Glucose uptake and mitochondrial activity of cell fractions within ascites (B) and tumor (C). Boxplots show medians (lines), interquartile range (box hinges) and range of data (box whiskers; excepting outliers, shown as points).

(D-E) Correlation between glucose uptake and mitochondrial activity of cell fractions within the ascites (D) and tumor (E).

(F-G) Correlation of glucose uptake (F) and mitochondrial activity (G) of cell fractions between ascites and tumor. Median (per phenotype) of median (per sample) biexponential-transformed Median Fluorescence Intensity (MFI) values shown.

### **fig. S3. Cell-specific metabolite profiling reveals changes in relative metabolite abundance**

(A) Heatmap of normalized metabolite abundance, with dendrograms representing Ward's clustering of Euclidean distances among samples.

(B-C) Relative abundance of adenosine (B) and L-kynurenine (C) measured by liquid chromatography tandem mass spectrometry (LC-MS/MS). Boxplots show medians (lines), interquartile range (box hinges) and range of data up to 1.5X interquartile range (box whiskers; outliers shown as points). P-values are determined using *limma* with patient as a random effect, as described in methods (\* $p < 0.05$ ).

### **fig. S4. Changes in relative metabolite abundance across cell types within the ascites and tumor.**

(A) Heatmap of normalized metabolite abundance, with dendrograms representing Ward's clustering of Euclidean distances among samples. Relative abundance of metabolites in the ascites (left) and tumor (right).

(B) Top four significantly differing metabolites across patients (all  $P_{adj}$  for F-Test of patient effect in *limma*  $< 0.05$ ). Boxplots show medians (lines), interquartile range (box hinges) range of data up to 1.5X interquartile range (box whiskers; excepting outliers, shown as points).

**fig. S5. Expression of population defining makers and metabolic genes within the scRNA-seq data.** Expression of *NNMT*, *CD3D*, *EPCAM*, *COL1A1*, *PTPRC*, *AOX1*, *CD8A*, *GZMA*, and *RPS12* within ascites and tumor, shown as log<sub>2</sub> normalized unique molecular identifier (UMI) counts. Data in (A) was obtained from samples from the BC Cancer Tumour Tissue Repository (n=3), and data from (B) was adapted from Izar *et al.* (n=6) (16) as described in the methods.